frontiers | Frontiers in Earth Science

TYPE Original Research
PUBLISHED 09 January 2023
DOI 10.3389/feart.2022.1032313

OPEN ACCESS

EDITED BY
Bo Sun,
Nanjing University of Information Science and Technology, China

REVIEWED BY
Zixuan Han,
Hohai University, China
Shaobo Qiao,
Sun Yat-sen University, China
Qin Wen,
Nanjing Normal University, China

*CORRESPONDENCE
Guolin Feng,
fenggl@cma.gov.cn

SPECIALTY SECTION
This article was submitted to Atmospheric Science, a section of the journal Frontiers in Earth Science

RECEIVED 30 August 2022
ACCEPTED 21 September 2022
PUBLISHED 09 January 2023

CITATION
Cheng J, Zhao Y, Zhi R and Feng G (2023), Meridional circulation dominates the record-breaking "Dragon Boat Water" rainfall over south China in 2022.
Front. Earth Sci. 10:1032313.
doi: 10.3389/feart.2022.1032313

Meridional circulation dominates the record-breaking "Dragon Boat Water" rainfall over south China in 2022

Jianbo Cheng[1], Yuheng Zhao[2], Rong Zhi[2] and Guolin Feng[3,4]*

[1]School of Environmental Science and Engineering, Yancheng Institute of Technology, Yancheng, China, [2]Laboratory for Climate Studies, National Climate Center, China Meteorological Administration, Beijing, China, [3]College of Physical Science and Technology, Yangzhou University, Yangzhou, China, [4]Southern Marine Science and Engineering Guangdong Laboratory (Zhuhai), Zhuhai, China

During the "Dragon Boat Water" season in 2022, record-breaking anomalous rainfall occurred over South China (SC). In this study, the causes of anomalous rainfall are investigated by using the novel moisture budget equation of three-pattern circulations. The results show that the anomalous rainfall over SC caused by the horizontal, meridional, and zonal circulations was −10 mm, 168 mm, and 45.3 mm, which contribute −5%, 86%, and 23% of the actual rainfall anomaly (195.1 mm), respectively, suggesting that the meridional circulation contributes most to anomalous rainfall, followed by zonal circulation, and horizontal circulation contributes negatively. Further analysis based on the three-pattern decomposition of the global atmospheric circulation shows that the spatial configuration of the anomalous horizontal circulation and vertical vorticity provides the background for generating the anomalous divergence and convergence of meridional and zonal circulations and further anomalous vertical velocity of the meridional and zonal circulations, ultimately resulting in anomalous rainfall.

KEYWORDS

record-breaking rainfall, "dragon boat water" season, south China, novel moisture budget equation, meridional circulation

1 Introduction

South China (SC) is located in the southernmost region of China, which comprises the southern region of the Yangtze River basin and the eastern region of the Tibetan Plateau; it includes the Guangdong, Guangxi, Hainan, and Fujian Provinces and their surrounding areas. SC has abundant rainfall that is characterized by a large annual mean value, high frequency of rainstorms, and long duration (Zhai and Eskridge, 1997; Yuan et al., 2010; Chu et al., 2018; Miao et al., 2019; Chu et al., 2020). According to the differences in influencing factors and time periods, the flood season of SC can be divided into two periods (Ramage, 1952; Yang and Sun, 2005; Yuan et al., 2019). The first flood season is generally called the "first rainy season" or "early rainy season" of China, which occurs from April to June. The second flood

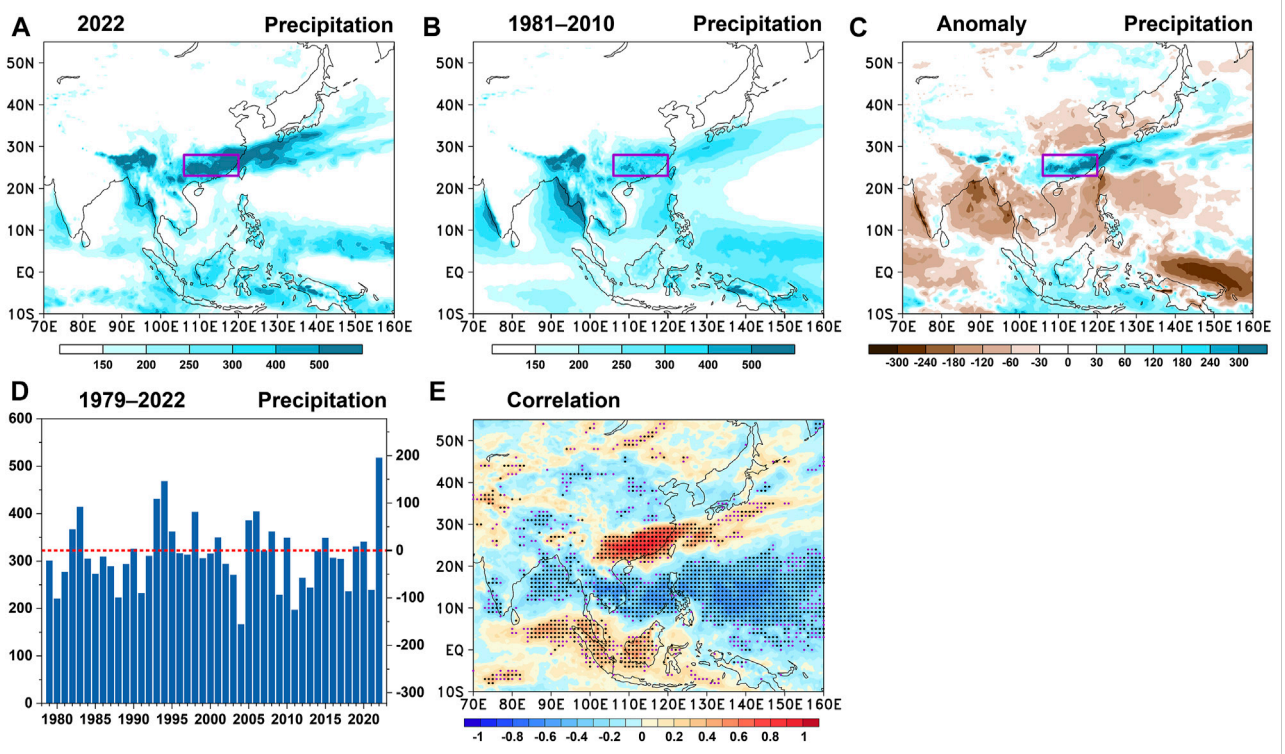

FIGURE 1
(A) Distribution of the accumulated rainfall during the "Dragon Boat Water" season (21 May to 20 June) in 2022; **(B)** and **(C)** are the same as **(A)** but for the climatological rainfall during 1981–2010 and the rainfall anomaly in 2022, respectively. The rainfall anomaly is calculated by subtracting the climatological rainfall during 1981–2010. The purple box in **(A–C)** represents the region of South China (SC; 106°E–120°E, 23°N–28°N). **(D)** Time series of the regionally averaged rainfall over SC during 1979–2022. The Y-axis on the left (right) represents the rainfall (rainfall anomaly). The red dashed line represents the climatological rainfall (zero line of rainfall anomaly) for the Y-axis on the left (right). **(E)** Correlation between the regionally averaged rainfall anomaly over SC and the rainfall anomaly during 1979–2022. Black (purple) dots over the shading represent that those correlation coefficients are significant above the 95% (90%) confidence level based on Student's t test. Units of the rainfall and rainfall anomaly are mm.

season is generally called the "second rainy season" or "late rainy season" of China, which occurs from July to September. In the first rainy season, the rainfall in SC is mainly influenced by monsoon circulations, including the subtropical jet, western Pacific subtropical high, South Asia high, and low-level southwest jet in the subtropics and the East Asian trough and northeastern cold vortex in the mid–high latitudes (Yuan et al., 2012; Li et al., 2018; Miao et al., 2019; Liu et al., 2022). In the second rainy season, the rainfall in SC is mainly influenced by typhoons or tropical depressions (Lee et al., 2010; Yuan et al., 2019).

During the first rainy season, there is a special time period called the "Dragon Boat Water" rainfall season. The name "Dragon Boat Water" rainfall season originates from 21 May to 20 June, which includes the Chinese Dragon Boat Festival (Lin et al., 2009; Gu and Zhang, 2012; Qian et al., 2020). During the "Dragon Boat Water" rainfall season, the rainfall is concentrated and generally accompanied by thunderstorms over SC. Climatically, the regionally averaged rainfall during the "Dragon Boat Water" season over SC (106°E–120°E, 23°N–28°N) is 322.3 mm (Figures 1B,D). In 2022, an extreme "Dragon Boat Water" rainfall occurred, with the regionally averaged rainfall reaching 517.5 mm, which is 1.6 times the climatological mean value and represents the highest record since 1979 (Figures 1A–D). Since extreme rainfall can lead to great socioeconomic losses, crop destruction, and casualties (Qiao et al., 2021), thus, the primary causes of the extreme rainfall during the "Dragon Boat Water" season should be studied. In addition to the record-breaking "Dragon Boat Water" rainfall, the zonal negative rainfall anomaly belt in the north and south of SC, the zonal positive rainfall anomaly belt in the Southern Hemisphere, and the negative rainfall anomaly in the east of the Malay Archipelago can be observed (Figure 1C). Further correlation analysis (Figure 1E) suggests that the anomalous "Dragon Boat Water" rainfall over SC is generally accompanied by the anomalous rainfall shown in Figure 1C, implying that the same anomalous atmospheric circulation system caused the anomalous rainfall in 2022 shown in Figure 1C.

According to previous studies (Seager et al., 2010; Han et al., 2021), the moisture budget equation can be used to investigate the relative contributions of anomalous atmospheric circulation (dynamic term) and anomalous moisture (thermodynamic term) to anomalous rainfall. Additionally, a novel decomposition of atmospheric circulation, which is called the three-pattern decomposition of global atmospheric circulation (3P-DGAC), can be used to explore anomalous atmospheric circulation (Liu et al., 2008; Hu et al., 2017; Hu et al., 2018a; Hu et al., 2018b; Hu et al., 2020). However, the quantitative contribution of the three-pattern circulations (i.e., horizontal, meridional, and zonal circulations) to anomalous rainfall cannot be obtained using the 3P-DGAC method. To solve this issue, Han et al. (2021) and Cheng et al. (2022) developed a novel moisture budget equation of the three-pattern circulations by incorporating the 3P-DGAC method into the moisture budget equation. Namely, the rainfall anomaly can be linked up with three-pattern circulations by using the novel moisture budget equation. By using the novel moisture budget equation, Cheng et al. (2022) studied the extreme rainfall in Henan Province in July 2021 and found that zonal circulation played the dominant role in causing this anomalous rainfall. In this study, the novel moisture budget equation of three-pattern circulations is adopted to investigate the relative contribution of the three-pattern circulations to the record-breaking "Dragon Boat Water" rainfall over SC in 2022.

This study is organized as follows. The study area, datasets, and methods used are described in Section 2. The quantitative contribution of the three-pattern circulations to anomalous rainfall is investigated using the novel moisture budget equation in Section 3. The anomalous three-pattern circulations and underlying mechanism are studied in Section 4. Finally, the summary and conclusion are given in Section 5.

2 Materials and methods

2.1 Study area

According to the spatial pattern of the anomalous rainfall during the "Dragon Boat Water" season in 2022 (Figure 1C), the study area of the SC in the present study is defined as (106°E–120°E, 23°N–28°N), which is shown as a purple box in Figure 1.

2.2 Source of data

The hourly rainfall, specific humidity, surface pressure, zonal wind, meridional wind, and vertical velocity from the European Center for Medium Range Weather Forecasts Reanalysis 5 (ERA5) (Hersbach et al., 2020) are used for the investigation in this study. The original horizontal resolution of these datasets is 0.25° × 0.25°, and we interpolate these datasets into the 0.5° × 0.5° horizontal resolution for this study. In the vertical direction, we adopt the commonly used 17 pressure levels, i.e., 1000, 925, 850, 700, 600, 500, 400, 300, 250, 200, 150, 100, 70, 50, 30, 20, and 10 hPa. We use the datasets during the "Dragon Boat Water" rainfall season (i.e., 21 May to 20 June) from 1979 to 2022.

2.3 Novel moisture budget equation of three-pattern circulations

Based on the moisture budget equation (Seager et al., 2010; Han et al., 2021) and the 3P-DGAC method (Liu et al., 2008; Hu et al., 2017; Hu et al., 2018a; Hu et al., 2018b; Cheng et al., 2018; Hu et al., 2020), Han et al. (2021) and Cheng et al. (2022) developed a novel moisture budget equation of three-pattern circulations as follows:

$$\delta P = \delta P\_H + \delta P\_M + \delta P\_Z + \delta R, \tag{1}$$

where δP represents the anomalous rainfall. δP_H, δP_M, and δP_Z represent the anomalous rainfall caused by the horizontal, meridional, and zonal circulations. δR represents the anomalous rainfall caused by the residual term. δ represents the difference during the "Dragon Boat Water" season between 2022 and the climatological mean of 1981–2010 in this study.

Since the novel moisture budget equation can be written as $\delta P = \delta MCDA + \delta MCDD + \delta THA + \delta THD + \delta R$, therefore, δP_H, δP_M, and δP_Z can be further decomposed as follows:

$$\begin{cases} \delta P\_H = \delta MCDA\_H + \delta MCDD\_H + \delta THA\_H + \delta THD\_H, \\ \delta P\_M = \delta MCDA\_M + \delta MCDD\_M + \delta THA\_M + \delta THD\_M, \\ \delta P\_Z = \delta MCDA\_Z + \delta MCDD\_Z + \delta THA\_Z + \delta THD\_Z, \end{cases} \tag{2}$$

where δMCDA and δMCDD represent anomalous rainfall caused by the change in advection and divergence to the dynamic term. δTHA and δTHD represent advection and divergence to the thermodynamic term. H, M, and Z on the right of each term represent that those terms are induced by the horizontal, meridional, and zonal circulations, respectively. δMCDA, δMCDD, δTHA, and δTHD can be represented as follows:

$$\begin{cases} \delta MCDA = -\frac{1}{\rho_w g}\int_{P_s}^{0}\left(\delta\vec{V}\cdot\nabla q_0\right)dp, \\ \delta MCDD = -\frac{1}{\rho_w g}\int_{P_s}^{0}\left(q_0\nabla\cdot\delta\vec{V}\right)dp,\Big)dp, \\ \delta THD = -\frac{1}{\rho_w g}\int_{P_s}^{0}\left(\overrightarrow{V_0}\cdot\nabla\delta q\right) \end{cases}$$

$$\delta THA = -\frac{1}{\rho_w g}\int_{P_s}^{0}\left(\overrightarrow{V_0}\cdot\nabla\delta q\right)dp, \tag{3}$$

where ρ_w, g, $\vec{V}$, and q represent the density of water, gravitational acceleration, horizontal wind, and specific humidity, respectively. Subscript 0 represents that the variables are the climatological

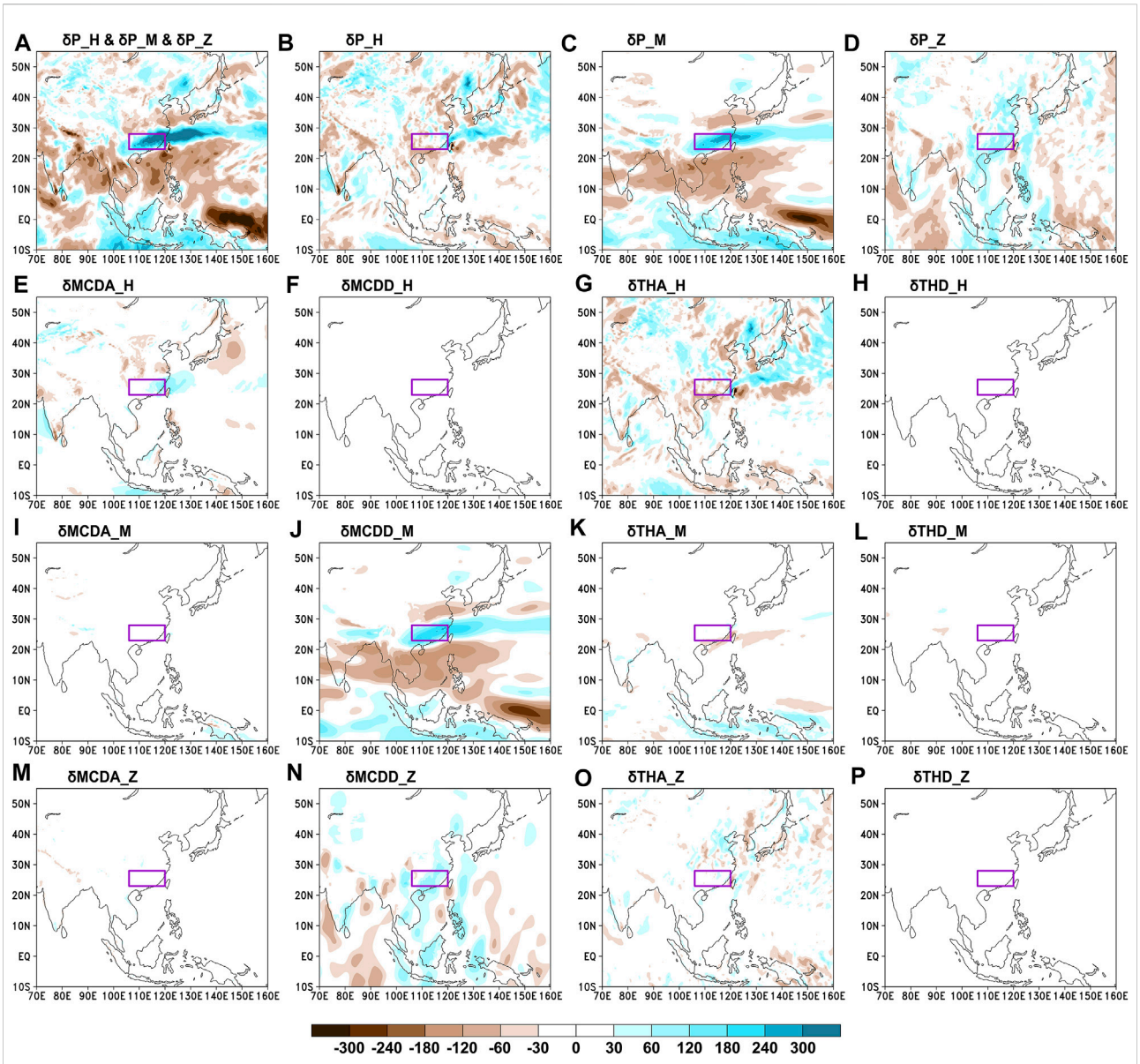

FIGURE 2
(A) Anomalous rainfall caused by the combined effects of horizontal (δP_H), meridional (δP_M), and zonal (δP_Z) circulations (i.e., δP_H + δP_M + δP_Z) during the "Dragon Boat Water" season in 2022 based on the novel moisture budget equation; **(B–D)** are the same as **(A)** but for the anomalous rainfall caused by the **(B)** horizontal, **(C)** meridional, and **(D)** zonal circulations. **(E–H)** Anomalous rainfall caused by the change in **(E)** advection (δMCDA_H) and **(F)** divergence (δMCDD_H) to the dynamic term and **(G)** advection (δTHA_H) and **(H)** divergence (δTHD_H) to the thermodynamic term induced by the horizontal circulation; **(I–L)** and **(M–P)** are the same as **(E–H)** but for those induced by the meridional and zonal circulations, respectively. **(I–L)** are δMCDA_M, δMCDD_M, δTHA_M, and δTHD_M, and **(M–P)** areδMCDA_Z, δMCDD_Z, δTHA_Z, and δTHD_Z. Units of the anomalous rainfall caused by changes in the moisture budget components are mm.

mean of 1981–2010. δMCDA, δMCDD, δTHA, and δTHD of the three-pattern circulations can be obtained using the corresponding anomalous horizontal wind in Eq. 3, i.e., $\delta\vec{V}_{\mathrm{H}}$ and $\vec{V}_{\mathrm{H0}}$ for the horizontal circulation, $\delta\vec{V}_{\mathrm{M}}$ and $\vec{V}_{\mathrm{M0}}$ for the meridional circulation, and $\delta\vec{V}_{\mathrm{Z}}$ and $\vec{V}_{\mathrm{Z0}}$ for the zonal circulation, respectively. The novel moisture budget equation of three-pattern circulations can be used to investigate the relative contribution of the three-pattern circulations to the record-breaking "Dragon Boat Water" rainfall over SC in 2022, which cannot be obtained by using the moisture budget equation or the 3P-DGAC method independently.

In the process of calculation, the δMCDA, δMCDD, δTHA, and δTHD of the three-pattern circulations are first calculated by using Eq. 3. Second, the anomalous rainfall caused by the horizontal,

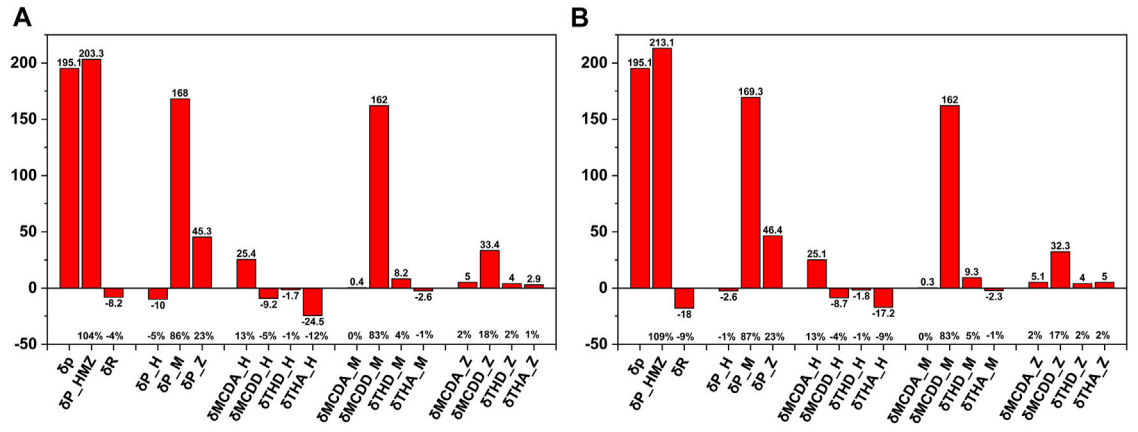

FIGURE 3
(A) Regionally averaged rainfall anomaly (δP) and the regionally averaged anomalous rainfall caused by changes in the moisture budget components over SC during the "Dragon Boat Water" season in 2022. δP_HMZ represents anomalous rainfall caused by the combined effects of horizontal, meridional, and zonal circulations (i.e., δP_H + δP_M + δP_Z). δR represents anomalous rainfall caused by the residual term. The physical meanings of the other terms are the same as those in Figure 2 but for the regionally averaged values. The percentages on the bottom represent the contributions of changes in the moisture budget components to δP. **(B)** is the same as **(A)** but for the results where the upper limit of vertical integration of Eq. 3 changes to 500 hPa. Units of the rainfall anomaly and anomalous rainfall caused by changes in the moisture budget components are mm.

meridional, and zonal circulations is calculated by using Eq. 2. Third, the residual term δR is calculated by using Eq. 1. More details of the 3P-DGAC method can be obtained in (Hu et al., 2017; Hu et al., 2018a; Hu et al., 2018b), and a detailed deduction of the novel moisture budget equation can be obtained in (Han et al., 2021; Cheng et al., 2022).

3 Quantitative contribution of the three-pattern circulations to anomalous rainfall

Figure 2A displays the spatial distribution of the anomalous rainfall caused by the combined effects of horizontal, meridional, and zonal circulations (i.e., δP_H + δP_M + δP_Z) during the "Dragon Boat Water" season in 2022. The spatial distribution of the anomalous rainfall caused by the three-pattern circulations is similar to the actual rainfall anomaly, with the spatial similarity coefficient reaching 0.74 (Figure 1C, Figure 2A). The anomalous rainfall over SC caused by the three-pattern circulations is 203.3 mm, which is equal to 104% of the actual rainfall anomaly (195.1 mm), while the anomalous rainfall caused by the residual term is −8.2 mm, which contributes −4% (Figure 3A), implying that the total rainfall change in 2022 can be largely explained by the sum of three-pattern circulations.

Figures 2B–D show the anomalous rainfall caused by the horizontal, meridional, and zonal circulations, respectively. By comparing Figures 2A,C, it can be observed that the anomalous rainfall caused by the meridional circulation is similar to that caused by the three-pattern circulations, and the spatial similarity coefficient between Figures 2A,C is 0.82. Additionally, by comparing Figures 2B–D, it can be observed that the meridional circulation contributes most to the anomalous rainfall, followed by zonal circulation, and the contribution of the horizontal circulation is the least, implying that the meridional circulation plays the dominant role in the anomalous rainfall. The quantitative anomalous rainfall over SC caused by the horizontal, meridional, and zonal circulations is −10 mm, 168 mm, and 45.3 mm, which contribute −5%, 86%, and 23% of the actual rainfall anomaly, respectively (Figure 3A).

Figures 2E–H show the anomalous rainfall caused by the change in advection (δMCDA_H) and divergence (δMCDD_H) to the dynamic term and changes in advection (δTHA_H) and divergence (δTHD_H) to the thermodynamic term induced by the horizontal circulation. By comparing Figures 2B,G, it can be observed that the anomalous rainfall caused by δTHA_H is similar to that caused by δP_H, and the spatial similarity coefficient between Figures 2B,G is 0.89, implying that δTHA_H contributes most to δP_H.

Figure 2I–L show the anomalous rainfall caused by δMCDA_M, δMCDD_M, δTHA_M, and δTHD_M. By comparing Figures 2C,J, it can be observed that the anomalous rainfall caused by δMCDD_M is similar to that caused by δP_M, and the spatial similarity coefficient between Figures 2C,J is 0.95, implying that δMCDD_M contributes most to δP_M. The quantitative anomalous rainfall over SC caused by δMCDA_M, δMCDD_M, δTHA_M, and δTHD_M is 0.4 mm, 162 mm, −2.6 mm, and 8.2 mm, which contributes 0%, 83%, −1%, and 4% of the actual rainfall anomaly, respectively (Figure 3A).

Figures 2M–P show the anomalous rainfall caused by δMCDA_Z, δMCDD_Z, δTHA_Z, and δTHD_Z. By comparing Figures 2D,N, it can be observed that the anomalous rainfall caused

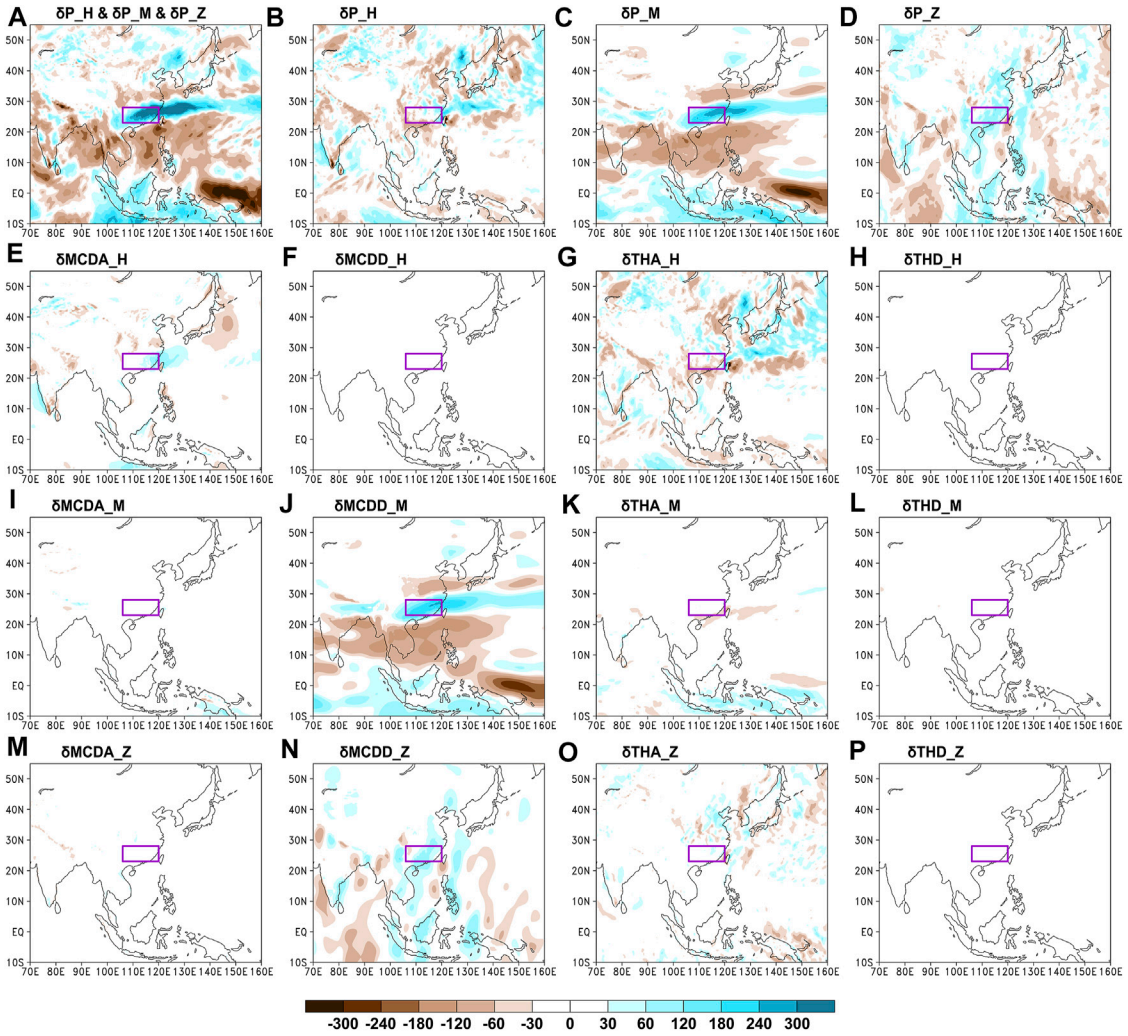

FIGURE 4
Figures 4A–P are the same as Figure 2A–P, except for that the results where the upper limit of vertical integration of Eq. 3 changes to 500 hPa.

by δMCDD_Z is similar to that caused by δP_Z, and the spatial similarity coefficient between Figures 2D,N is 0.79, implying that δMCDD_Z contributes most to δP_Z. The quantitative anomalous rainfall over SC caused by δMCDA_Z, δMCDD_Z, δTHA_Z, and δTHD_Z is 5 mm, 33.4 mm, 2.9 mm, and 4 mm, which contributes 2%, 18%, 1%, and 2% of the actual rainfall anomaly, respectively (Figure 3A).

Since the moisture mainly exists below 500 hPa (Supplementary Figure S1), the results where the upper limit of vertical integration of Eq. 3 changes to 500 hPa are similar to those obtained from Eq. 3 (comparing Figure 2, Figure 4). Additionally, the main conclusions of the quantitative contribution of the three-pattern circulations to the anomalous rainfall do not change (comparing Figures 3A,B).

Generally, δP_M (meridional circulation) contributes most to anomalous rainfall over SC, δP_Z (zonal circulation) follows, and δP_H (horizontal circulation) contributes negatively. Additionally, the main contributors to δP_H, δP_M, and δP_Z are δTHA_H, δMCDD_M, and δMCDD_Z, respectively.

4 Anomalous three-pattern circulations and underlying mechanism

4.1 Anomalous meridional and zonal circulations

Figures 5A–C display the total vertical velocity anomaly and the vertical velocity anomaly of meridional and zonal circulations, respectively, during the "Dragon Boat Water" season in 2022. Figure 5A shows that there exists a zonal negative velocity anomaly belt over SC, implying that there is

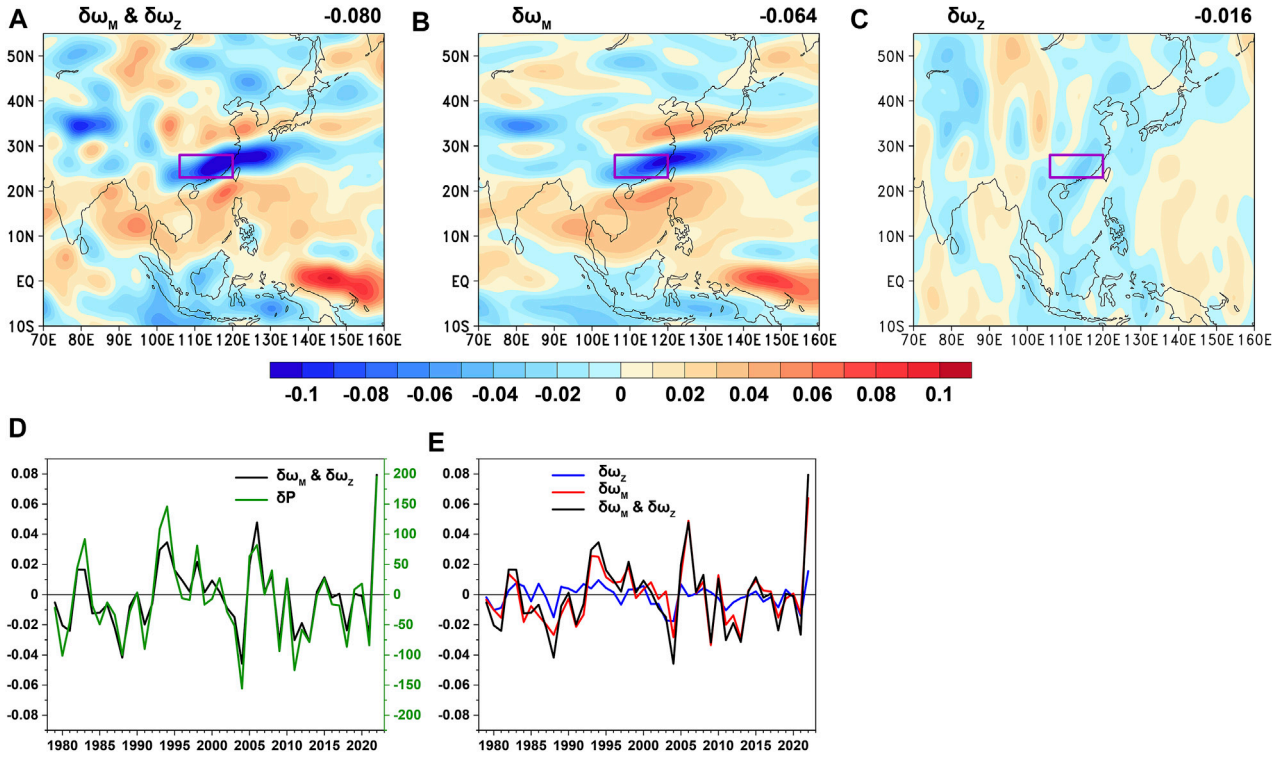

FIGURE 5
(A) Distribution of the vertical velocity anomaly during the "Dragon Boat Water" season in 2022; **(B)** and **(C)** are the same as **(A)** but for the vertical velocity anomaly of **(B)** meridional and **(C)** zonal circulations, respectively. Positive (negative) values in **(A–C)** represent sinking (rising) motion. The values in the upper right corners of **(A–C)** represent the regionally-averaged vertical velocity anomalies over SC. **(D)** Time series of the regionally-averaged vertical velocity anomaly (black line) and rainfall anomaly (green line) over SC during 1979–2022. The Y-axis on the left (right) represents the vertical velocity (rainfall) anomaly. **(E)** Time series of the regionally-averaged vertical velocity anomaly (black line) and vertical velocity anomaly of meridional (red line) and zonal (blue line) circulations over SC during 1979–2022. Vertical velocity anomalies in **(D)** and **(E)** are multiplied by −1 for convenience. Units of the vertical velocity anomaly and rainfall anomaly are Pa s^{-1} and mm, respectively.

anomalous rising motion over SC. Additionally, the zonal positive velocity anomaly belt in the north and south of SC, the zonal negative velocity anomaly belt in the Southern Hemisphere, and the positive velocity anomaly in the east of the Malay Archipelago can be observed. Comparing Figure 1C, Figure 5A, the spatial patterns of the vertical velocity anomaly and rainfall anomaly are similar, and the spatial similarity coefficient is −0.76, implying that the anomalous rainfall is caused by the anomalous vertical velocity of meridional and zonal circulations. This result is also supported by Figure 5D since the correlation between the time series of the regionally averaged vertical velocity anomaly (multiplied by −1) and rainfall anomaly over SC during 1979–2022 reaches 0.95. Therefore, the extremely anomalous vertical velocity over SC leads to record-breaking "Dragon Boat Water" rainfall in 2022 (Figure 5D).

Figures 5A,B show that the spatial patterns of the total vertical velocity anomaly and vertical velocity anomaly of meridional circulation are similar. Additionally, the regionally-averaged vertical velocity anomaly of the meridional circulation over SC is −0.064 Pa s^{-1}, which contributes 80% of the total vertical velocity anomaly (−0.08 Pa s^{-1}), while the regionally-averaged vertical velocity anomaly of the zonal circulation is −0.016 Pa s^{-1}, which contributes 20% of the total vertical velocity anomaly (Figure 5E). The results proposed above are similar to those obtained from the novel moisture equations. This is because the vertical velocity anomalies of meridional and zonal circulations are closely related to δMCDD_M and δMCDD_Z, which are the main contributors to the anomalous rainfall, as shown in Figure 2, Figure 4. This proposal can be proven by the following deduction. According to Eq. 3, δMCDD_M and δMCDD_Z can be written as follows:

$$\begin{cases} \delta\text{MCDD\_M} = -\dfrac{1}{\rho_w g}\displaystyle\int_{P_s}^{0}(q_0\nabla\cdot\delta\vec{V}_{\text{M}})dp, \\ \delta\text{MCDD\_Z} = -\dfrac{1}{\rho_w g}\displaystyle\int_{P_s}^{0}(q_0\nabla\cdot\delta\vec{V}_{\text{Z}})dp. \end{cases} \tag{4}$$

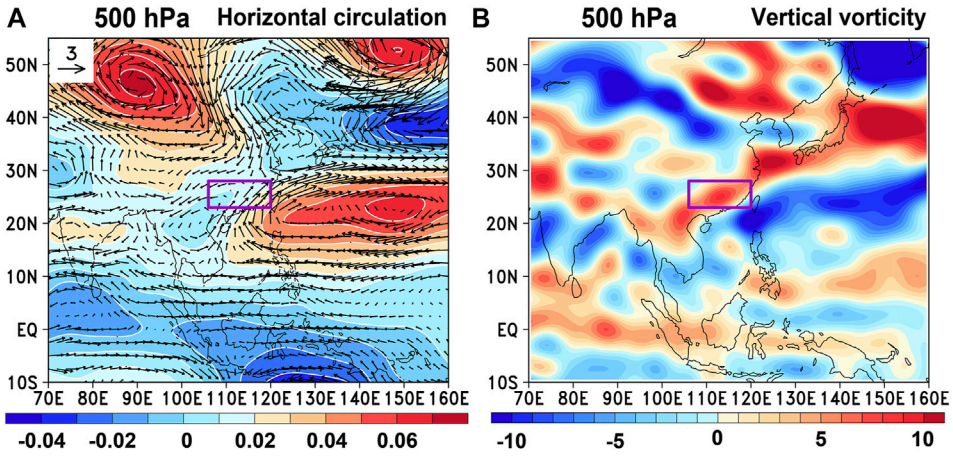

FIGURE 6
(A) Distribution of the horizontal circulation anomaly at 500 hPa during the "Dragon Boat Water" season in 2022. Shading and vector represent the stream function anomaly and wind anomaly of the horizontal circulation; **(B)** is the same as **(A)** but for the distribution of the vertical vorticity anomaly of horizontal circulation at 500 hPa. Units of the stream function, wind, and vorticity anomalies are 10^{-6} s^{-1}, m s^{-1}, and 10^{-6} s^{-1}, respectively.

Since the specific humidity mainly exists below 500 hPa, Eq. 4 can be rewritten as follows:

$$\begin{cases} \delta\text{MCDD\_M} \approx -\dfrac{1}{\rho_w g}\displaystyle\int_{P_s}^{500hPa}(q_0\nabla\cdot\delta\vec{V}_{\text{M}})dp, \\ \delta\text{MCDD\_Z} \approx -\dfrac{1}{\rho_w g}\displaystyle\int_{P_s}^{500hPa}(q_0\nabla\cdot\delta\vec{V}_{\text{Z}})dp. \end{cases} \tag{5}$$

The deduction from Eq. 4, to Eq. 5 can be confirmed by Figure 2, Figure 4. Since q_0 represents the climatological specific humidity during 1981–2010, δMCDD_M and δMCDD_Z are mainly controlled by $-\int_{P_s}^{500hPa}\nabla\cdot\delta\vec{V}_{\text{M}}\text{dp}$ and $-\int_{P_s}^{500hPa}\nabla\cdot\delta\vec{V}_{\text{Z}}\text{dp}$. According to the 3P-DGAC method, the meridional circulation $\vec{V}_{\text{M}}=\vec{j}v_{\text{M}}+\vec{k}\omega_{\text{M}}$ and zonal circulation $\vec{V}_{\text{Z}}=\vec{i}u_{\text{Z}}+\vec{k}\omega_{\text{Z}}$ satisfy the two continuity equations as follows:

$$\begin{cases} \dfrac{1}{a\cos\varphi}\dfrac{\partial v_{\text{M}}}{\partial\lambda}+\dfrac{\partial\omega_{\text{M}}}{\partial p}=0, \\ \dfrac{1}{a}\dfrac{\partial u_{\text{Z}}}{\partial\varphi}+\dfrac{\partial\omega_{\text{Z}}}{\partial p}=0. \end{cases} \tag{6}$$

The continuity equations can be rewritten as follows:

$$\begin{cases} \dfrac{\partial\omega_{\text{M}}}{\partial p}=-\dfrac{1}{a\cos\varphi}\dfrac{\partial v_{\text{M}}}{\partial\lambda}, \\ \dfrac{\partial\omega_{\text{Z}}}{\partial p}=-\dfrac{1}{a}\dfrac{\partial u_{\text{Z}}}{\partial\varphi}. \end{cases} \tag{7}$$

Therefore, the vertical velocity of the meridional and zonal circulations at 500 hPa can be calculated as follows:

$$\begin{cases} \omega_{\text{M}}=-\displaystyle\int_{P_s}^{500hPa}\frac{1}{a\cos\varphi}\frac{\partial v_{\text{M}}}{\partial\lambda}dp=-\int_{P_s}^{500hPa}\nabla\cdot\vec{V}_{\text{M}}dp, \\ \omega_{\text{Z}}=-\displaystyle\int_{P_s}^{500hPa}\frac{1}{a}\frac{\partial u_{\text{Z}}}{\partial\varphi}dp=-\int_{P_s}^{500hPa}\nabla\cdot\vec{V}_{\text{Z}}dp. \end{cases} \tag{8}$$

Thus, the vertical velocity anomaly of the meridional and zonal circulations at 500 hPa can be obtained by using the following equations:

$$\begin{cases} \delta\omega_{\text{M}}=-\displaystyle\int_{P_s}^{500hPa}\nabla\cdot\delta\vec{V}_{\text{M}}dp, \\ \delta\omega_{\text{Z}}=-\displaystyle\int_{P_s}^{500hPa}\nabla\cdot\delta\vec{V}_{\text{Z}}dp. \end{cases} \tag{9}$$

Since δMCDD_M and δMCDD_Z are the main contributors to anomalous rainfall (Figure 2, Figure 4) and δMCDD_M and δMCDD_Z are mainly controlled by $-\int_{P_s}^{500hPa}\nabla\cdot\delta\vec{V}_{\text{M}}\text{dp}$ and $-\int_{P_s}^{500hPa}\nabla\cdot\delta\vec{V}_{\text{Z}}\text{dp}$ (i.e., $\delta\omega_{\text{M}}$ and $\delta\omega_{\text{Z}}$ at 500 hPa), the spatial patterns of the vertical velocity anomaly and the rainfall anomaly are similar. Additionally, the similarity between the quantitative contributions of the meridional and zonal circulations to the vertical velocity anomaly and those to the anomalous rainfall can also be explained.

4.2 Anomalous horizontal circulation

As proposed in the previous section, anomalous rainfall is caused by the anomalous vertical velocity of meridional and zonal

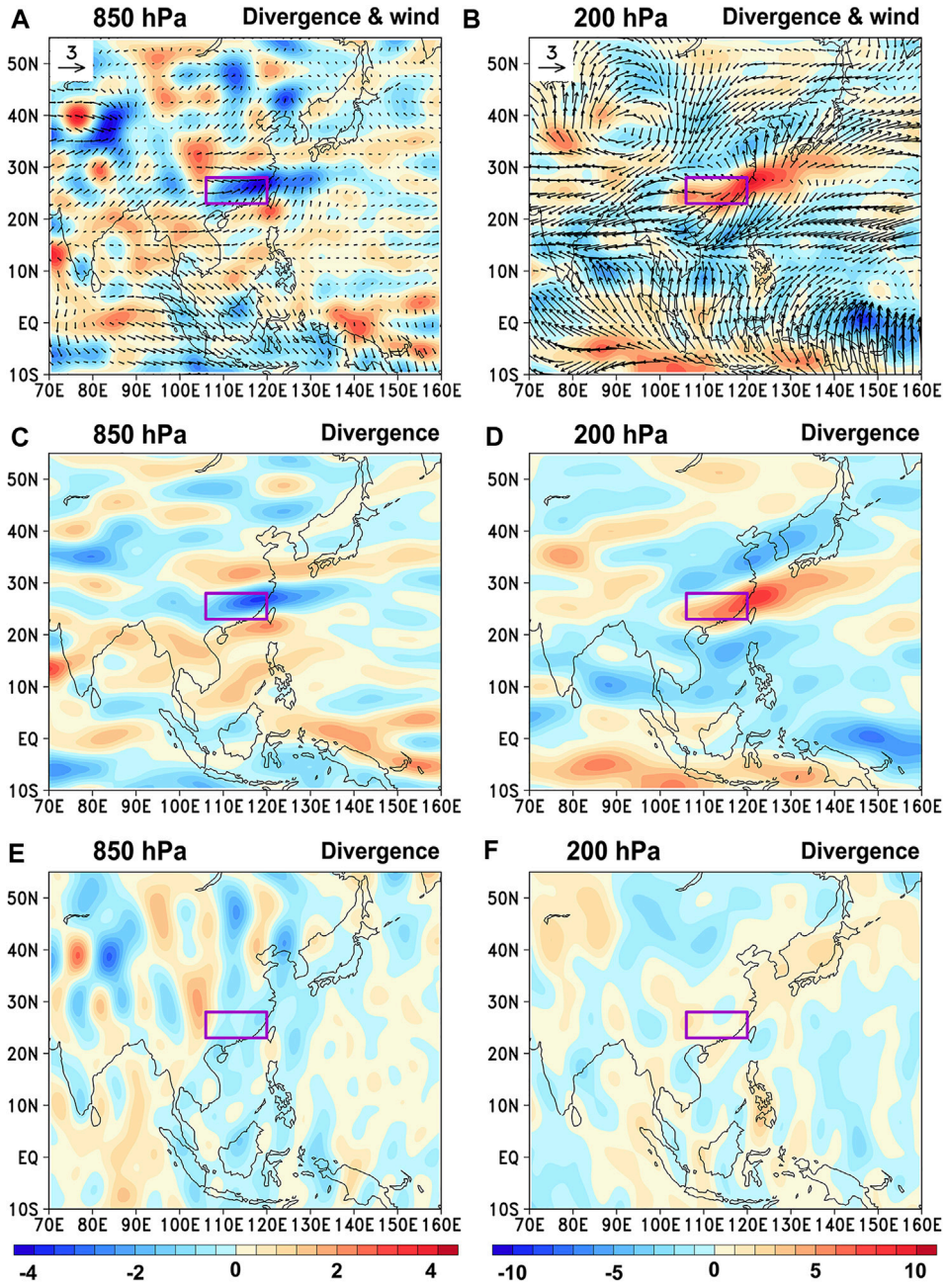

FIGURE 7
(A),(B) Distribution of the divergence anomaly (shading) and wind anomaly (vector) of the vertical circulation (i.e., the meridional and zonal circulations) at **(A)** 850 hPa and **(B)** 200 hPa during the "Dragon Boat Water" season in 2022; **(C),(D)** and **(E),(F)** are the same as **(A),(B)** but for the distribution of the divergence anomaly of the meridional and zonal circulations, respectively. Units of the divergence and wind anomalies are 10^{-6} s^{-1} and m s^{-1}, respectively.

circulations; thus, the cause of the anomalous vertical velocity is investigated in this section. Figure 6 displays the horizontal circulation anomaly and vorticity anomaly at 500 hPa during the "Dragon Boat Water" season in 2022. Figure 6 shows that affected by the continental high, anomalous anticyclonic circulation and negative vorticity exist over the region north of SC, which can result in anomalous divergence (convergence) in the lower (higher) troposphere (Figures 7A,B) and further anomalous sinking motion (Figure 5A). Over SC, affected by the anomalous continental high, anticyclonic circulation in the western Pacific,

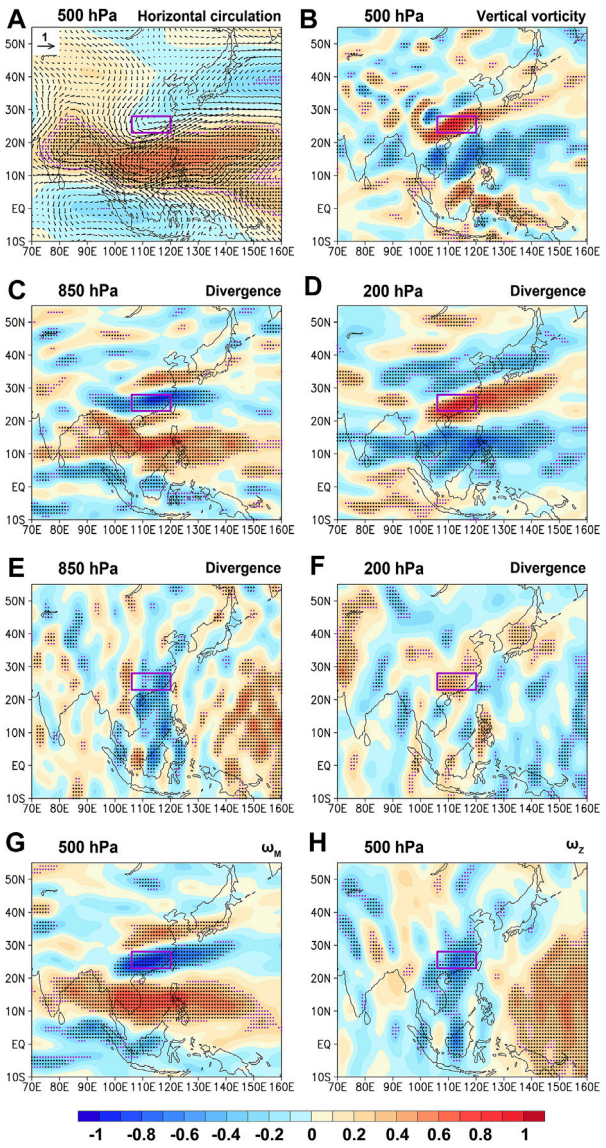

FIGURE 8
Correlation between the regionally averaged rainfall anomaly over SC and different variables during 1979–2022. **(A)** Horizontal circulation anomaly at 500 hPa. Shading and vector are for the stream function anomaly and wind anomaly of the horizontal circulation. **(B)** Vertical vorticity anomaly of horizontal circulation at 500 hPa. **(C),(D)** Divergence anomaly of meridional circulation at **(C)** 850 hPa and **(D)** 200 hPa. **(E),(F)** are the same as **(C),(D)** but for the zonal circulation. **(G),(H)** Vertical velocity anomaly of the **(G)** meridional and **(H)** zonal circulations at 500 hPa. Black (purple) dots over the shading represent that those correlation coefficients are significant above the 95% (90%) confidence level based on Student's t test.

and the trough north of the western Pacific anticyclone, anomalous cyclonic circulation and positive vorticity exist, which can result in anomalous convergence (divergence) in the lower (higher) troposphere and further anomalous rising motion. In the western Pacific and the area southeast of southern India, anomalous anticyclonic circulation and negative vorticity exist, which can result in anomalous divergence (convergence) in the lower (higher) troposphere and further anomalous sinking motion. Between 5°S and 5°N, except for the region east of the Malay Archipelago, anomalous cyclonic circulation and positive vorticity exist, which can result in anomalous convergence (divergence) in the lower (higher) troposphere and further anomalous rising motion. Generally, the spatial configuration of the anomalous horizontal circulation provides the background for the generation of the anomalous vertical velocity.

Additionally, the anomalous divergence of the meridional circulation is similar to that of the vertical circulation (i.e., meridional and zonal circulations) and is larger than that of the zonal circulation (Figures 7A–F), which corresponds to the dominant role of meridional circulation in influencing anomalous rainfall during the "Dragon Boat Water" season in 2022.

4.3 Correlation analysis

To verify the mechanism proposed above, correlation analysis is conducted. Figure 8 displays the correlation maps between the regionally averaged rainfall anomaly over SC and different variables during 1979–2022. By comparing Figure 8A, Figure 6A, the main characteristics of the spatial configuration are found to be similar, i.e., the anomalous continental high and the trough north of the western Pacific anticyclone in the mid–high latitudes, the anomalous anticyclonic circulation over the western Pacific and the area southeast of southern India in the subtropics, and the anomalous cyclonic circulation south of 5°N. The similarity of the spatial configurations of the anomalous horizontal circulation also leads to the similar spatial configuration of the vertical vorticity (Figure 8B, Figure 6B). Furthermore, the spatial configuration of the anomalous horizontal circulation and vertical vorticity leads to the anomalous divergence of meridional and zonal circulations (Figures 8C–F and Figures 7C–F) and further anomalous vertical velocity of the meridional and zonal circulations (Figures 8G,H and Figures 5B,C), which finally results in anomalous rainfall (Figure 1E). Additionally, the similarity between Figure 1E, Figure 8G corresponds to the findings that the meridional circulation dominates the anomalous rainfall during the "Dragon Boat Water" season in 2022.

5 Summary and conclusion

During the "Dragon Boat Water" season in 2022, record-breaking anomalous rainfall existed over SC and was accompanied by the zonal negative rainfall anomaly belt in the north and south of SC, the zonal positive rainfall anomaly belt in the Southern Hemisphere, and the negative rainfall anomaly in the east of the Malay Archipelago. In this study,

the causes of anomalous rainfall are investigated by using the novel moisture budget equation of three-pattern circulations, and the following conclusions are obtained.

(1) The anomalous rainfall over the SC caused by the horizontal (δP_H), meridional (δP_M), and zonal (δP_Z) circulations are −10 mm, 168 mm, and 45.3 mm, which contribute −5%, 86%, and 23% of the actual rainfall anomaly (195.1 mm), respectively, suggesting that δP_M contributes most to anomalous rainfall, δP_Z follows, and δP_H contributes negatively.
(2) The dynamic terms caused by the anomalous divergence of meridional (δMCDD_M) and zonal (δMCDD_Z) circulations are the main contributors to δP_M and δP_Z, while the thermodynamic term caused by the anomalous vapor advection of horizontal circulation (δTHA_H) is the main contributor to δP_H.
(3) Since δMCDD_M and δMCDD_Z are largely determined by the anomalous vertical velocity of the meridional and zonal circulations according to the novel moisture budget equation and continuity equation, and δMCDD_M and δMCDD_Z are the main contributors to anomalous rainfall, the anomalous vertical velocity leads to anomalous rainfall.
(4) The spatial configuration of the anomalous horizontal circulation and vertical vorticity provides the background for the generation of the anomalous divergence of meridional and zonal circulations and further the anomalous vertical velocity of the meridional and zonal circulations, ultimately resulting in anomalous rainfall.

It should be noted that the external forcings that cause anomalous horizontal, meridional, and zonal circulations are not investigated in this study and should be explored in the future.

Data availability statement

The original contributions presented in the study are included in the article/Supplementary Material, further inquiries can be directed to the corresponding author.

Author contributions

YZ and JC: methodology. YZ, JC, RZ, and GF: writing original draft preparation. YZ and JC: visualization. All authors contributed to the article and approved the submitted version.

Funding

This work was funded by National Natural Science Foundation of China (42130610, 42005012, 41975088), Natural Science Foundation of Jiangsu Province (BK20201058), and School-level research projects of Yancheng Institute of Technology (xjr2020022).

Conflict of interest

The authors declare that the research was conducted in the absence of any commercial or financial relationships that could be construed as a potential conflict of interest.

Publisher's note

Supplementary material

The Supplementary Material for this article can be found online at: https://www.frontiersin.org/articles/10.3389/feart.2022.1032313/full#supplementary-material

References

Cheng, J., Gao, C., Hu, S., and Feng, G. (2018). High-stability algorithm for the three-pattern decomposition of global atmospheric circulation. *Theor. Appl. Climatol.* 133, 851–866. doi:10.1007/s00704-017-2226-2

Cheng, J., Zhao, Y., Zhi, R., and Feng, G. (2022). Analysis of the July 2021 extreme precipitation in Henan using the novel moisture budget equation. *Theor. Appl. Climatol.* 149, 15–24. doi:10.1007/s00704-022-04022-7

Chu, Q., Wang, Q., and Feng, G. (2020). The roles of moisture transports in intraseasonal precipitation during the preflood season over South China. *Int. J. Climatol.* 40, 2239–2252. doi:10.1002/joc.6329

Chu, Q., Wang, Q., Qiao, S., and Feng, G. (2018). Feature analysis and primary causes of pre-flood season "Cumulative Effect" of torrential rain over South China. *Theor. Appl. Climatol.* 131, 91–100. doi:10.1007/s00704-016-1947-y

Gu, D., and Zhang, W. (2012). The strong dragon-boat race precipitation of Guangdong in 2008 and qusi-10-day oscillation. *J. Trop. Meteorology* 3, 349. (in Chinese)

Han, Z., Zhang, Q., Li, Q., Feng, R., Haywood, A. M., Tindall, J. C., et al. (2021). Evaluating the large-scale hydrological cycle response within the pliocene model intercomparison project phase 2 (PlioMIP2) ensemble. *Clim. Past.* 17, 2537–2558. doi:10.5194/cp-17-2537-2021

Hersbach, H., Bell, B., Berrisford, P., Hirahara, S., Horányi, A., MuñozSabater, J., et al. (2020). The ERA5 global reanalysis. *Q. J. R. Meteorol. Soc.* 146, 1999–2049. doi:10.1002/qj.3803

Hu, S., Cheng, J., and Chou, J. (2017). Novel three-pattern decomposition of global atmospheric circulation: Generalization of traditional two dimensional decomposition. *Clim. Dyn.* 49, 3573–3586. doi:10.1007/s00382-017-3530-3

Hu, S., Cheng, J., Xu, M., and Chou, J. (2018). Three-pattern decomposition of global atmospheric circulation: Part II—dynamical equations of horizontal, meridional and zonal circulations. *Clim. Dyn.* 50, 2673–2686. doi:10.1007/s00382-017-3763-1

Hu, S., Chou, J., and Cheng, J. (2018). Three-pattern decomposition of global atmospheric circulation: Part I—decomposition model and theorems. *Clim. Dyn.* 50, 2355–2368. doi:10.1007/s00382-015-2818-4

Hu, S., Zhou, B., Gao, C., Xu, Z., Wang, Q., and Chou, J. (2020). Theory of three-pattern decomposition of global atmospheric circulation. *Sci. China Earth Sci.* 63, 1248–1267. doi:10.1007/s11430-019-9614-y

Lee, M. H., Ho, C. H., and Kim, J. H. (2010). Influence of tropical cyclone landfalls on spatiotemporal variations in typhoon season rainfall over South China. *Adv. Atmos. Sci.* 27, 443–454. doi:10.1007/s00376-009-9106-3

Li, G., Chen, J., Wang, X., Luo, X., Yang, D., Zhou, W., et al. (2018). Remote impact of North Atlantic sea surface temperature on rainfall in southwestern China during boreal spring. *Clim. Dyn.* 50, 541–553. doi:10.1007/s00382-017-3625-x

Lin, L., Wu, N., Huang, Z., and Cai, A. (2009). Causality analysis of the infrequent dragon-boat precipitation in Guangdong province in 2008. *Meteorol. Mon.* 35, 43. (in Chinese)

Liu, F., Wang, B., Ouyang, Y., Wang, H., Qiao, S., Chen, G., et al. (2022). Intraseasonal variability of global land monsoon precipitation and its recent trend. *npj Clim. Atmos. Sci.* 5, 30. doi:10.1038/s41612-022-00253-7

Liu, H., Hu, S., Xu, M., and Chou, J. (2008). Three-dimensional decomposition method of global atmospheric circulation. *Sci. China Ser. D-Earth. Sci.* 51, 386–402. doi:10.1007/s11430-008-0020-9

Miao, R., Wen, M., Zhang, R., and Li, L. (2019). The influence of wave trains in mid-high latitudes on persistent heavy rain during the first rainy season over South China. *Clim. Dyn.* 53, 2949–2968. doi:10.1007/s00382-019-04670-y

Qian, W., Ai, Y., Chen, L., and Li, H. (2020). Anomalous synoptic pattern of typical dragon boat precipitation process in Guangdong province. *J. Trop. Meteorology* 36, 433. (in Chinese)

Qiao, S., Chen, D., Wang, W., Cheung, H. N., Liu, F., Cheng, J., et al. (2021). The longest 2020 Meiyu season over the past 60 years: Subseasonal perspective and its predictions. *Geophys. Res. Lett.* 48, e2021GL093596. doi:10.1029/2021GL093596

Ramage, C. S. (1952). Variation of rainfall over South China through the wet season. *Bull. Am. Meteorol. Soc.* 33, 308–311. doi:10.1175/1520-0477-33.7.308

Seager, R., Naik, N., and Vecchi, G. A. (2010). Thermodynamic and dynamic mechanisms for large-scale changes in the hydrological cycle in response to global warming. *J. Clim.* 23, 4651–4668. doi:10.1175/2010JCLI3655.1

Yang, H., and Sun, S. (2005). The characteristics of longitudinal movement of the subtropical high in the Western Pacific in the pre-rainy season in South China. *Adv. Atmos. Sci.* 22, 392–400. doi:10.1007/BF02918752

Yuan, C., Liu, J., Luo, J. J., and Guan, Z. (2019). Influences of tropical Indian and Pacific oceans on the interannual variations of precipitation in the early and late rainy seasons in South China. *J. Clim.* 32, 3681–3694. doi:10.1175/JCLI-D-18-0588.1

Yuan, F., Wei, K., Chen, W., Fong, S., and Leong, K. (2010). Temporal variations of the frontal and monsoon storm rainfall during the first rainy season in South China. *Atmos. Ocean. Sci. Lett.* 3, 243–247. doi:10.1080/16742834.2010.11446876

Yuan, Y., Ren, F., Wang, Y., Sun, L., and Guo, Y. (2012). Analysis of the precipitation feature and general circulation anomaly during the pre-flood season in South China in 2012. *Meteorol. Mon.* 38, 1247. (in Chinese)

Zhai, P., and Eskridge, R. E. (1997). Atmospheric water vapor over China. *J. Clim* 10, 26432–32652. doi:10.1175/1520-0442(1997)010<2643:AWVOC>2.0